6-1-1986

Experimental Measurements of Phase Space

Roger McWilliams
University of California, Irvine

D. P. Sheehan
University of San Diego, dsheehan@sandiego.edu

Experimental Measurements of Phase Space

Roger McWilliams and Daniel Sheehan
Department of Physics, University of California, Irvine, California 92717
(Received 28 February 1986)

Direct measurements of integrated phase-space densities, e.g., $f(x, v_y, t)$, have been made in an experiment. Using spectroscopically active ions, measurements in a plasma show the ion response, $f_i(\mathbf{x}, \mathbf{v}, t)$, to linear and nonlinear waves and phase-space particle bunching. Time-resolved measurements show coherent and incoherent phase-space density changes in the presence of waves, indicating that transitions to turbulence and chaos may be studied. The time, space, and velocity-space resolution may allow experimental tests of predictions from the Boltzmann equation.

PACS numbers: 52.25.Kn, 05.20.−y, 05.45.+b, 47.25.Ae

In this Letter we report direct experimental measurements of integrated phase-space densities. The measurements allowed phase-space densities integrated over two velocity components in physical-velocity space to be determined. The measuring technique was nonperturbing and did not require inference from the use of derivatives of the data. Resolution of about 2.0 μsec, 10^{-3} cm^3 and 3×10^{10} cm^3/sec^3 in time, space, and velocity space were obtained. Measurements were made on spectroscopically active ions in a plasma. Ion responses to small- and large-amplitude waves were observed, showing coherent and incoherent time-resolved responses, and indicating that transitions to turbulence and chaos may be studied. Additionally, phase-space particle bunching was observed.

Many differential equations arising in physics have solutions of the form $\psi=\psi(\mathbf{x}, \mathbf{v}, t)$, that is, the solutions are phase-space density functions. Moments of these functions yield information such as number density, momentum density, energy density, etc. Among important equations in statistical physics are the Boltzmann equations, which can be written for plasmas

$$\frac{\partial f_j}{\partial t}+\mathbf{v}\cdot\nabla f_j+\frac{q_j}{m_j}\left(\mathbf{E}+\frac{\mathbf{v}\times\mathbf{B}}{c}\right)\cdot\frac{\partial f_j}{\partial \mathbf{v}}=\left.\frac{df_j}{dt}\right|_{\text{collisions}}, \quad (1)$$

predicting the dependence of the jth-particle distribution function $f_j(\mathbf{x}, \mathbf{v}, t)$ on charge, mass, space, velocity, collisions, and electromagnetic fields.

Experimentalists commonly can measure number density along with electromagnetic field quantities, but a direct measure of f is difficult to achieve. The motion of number-density "blobs" has been reported.[1] Energy analyzers have been used with increasing success,[2,3] but still suffer from two drawbacks. Firstly, the analyzer usually is physically larger than many distance scales of interest and perturbs the measured system. Secondly, commonly in laboratory experiments the distribution function is obtained by differentiation of an integrated flux measurement, a technique requiring considerable caution (especially when the analyzer acceptance angle is large). Theorists have predicted wave-particle trapping,[4] bunching,[5] routes to turbulence,[6–8] and phase-space clumps.[9,10] An experimental test of a stochastic theory has been reported.[11]

Phase-space coordinates for Eq. (1) involve three physical-space dimensions and three velocity-space dimensions. The experiments reported here are of measurements of integrated phase-space density presented in a planar view involving one physical-space dimension and one velocity-space dimension, having been integrated over the two velocity components perpendicular to the velocity-space dimension displayed. For example, measurements were made of

$$f_i(x, v_y, t)\equiv\int f_i(x,y,z, v_x, v_y, v_z, t)\,dv_x\,dv_z, \quad (2)$$

with y and z fixed. Each individual scan thus represents a partially integrated distribution function similar to that obtainable with a plane electrostatic probe. A set of these measurements throughout the physical- and velocity-space regions of interest along with electromagnetic field data may allow testing of features predicted by the Boltzmann equation. In particular, a set of scans at various angles in velocity space allows the complete, nonintegrated $f_i(\mathbf{x}, \mathbf{v}, t)$ to be obtained by use of tomographic reconstruction techniques.[12]

Phase-space densities were measured via laser-induced fluorescence techniques,[13] as shown schematically in Fig. 1. A tunable dye laser induces a transition to an excited state in a target particle when the laser frequency is tuned to the necessary Doppler-shifted resonance frequency for the moving target particle. The target particle then emits a photon which is gathered through collection optics. The spatial resolution of the collimated laser beam and collection optics is 1 mm^3. The velocity resolution is limited only by the natural linewidth of the absorption line, corresponding to an uncertainty of about 3×10^{10} cm^3/sec^3 in three-dimensional velocity space or about 3×10^3 cm/sec in speed. For this experiment sufficient photons are collected (by means of a boxcar technique) for a time resolution of 2.0 μsec.

The experiments reported here were performed in a single-ended Q machine[14] (see Fig. 1) which provided

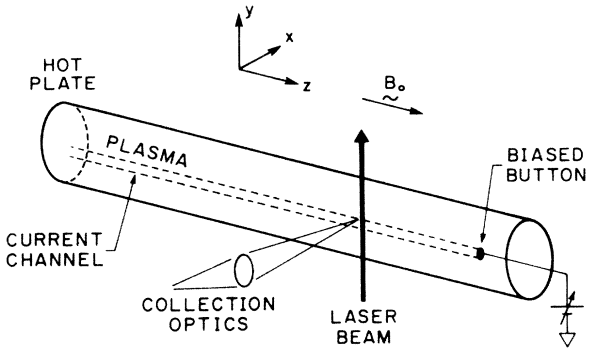

FIG. 1. Schematic of experimental apparatus showing cylindrical plasma, the channel through which an electron current is drawn to the button (which creates instability), and the movable laser beam with detection optics for phase-space density measurements.

a low-density ($n \sim 5\times10^9$ cm^{-3}), low-temperature ($T_i \approx T_e \approx 0.2$ eV), nearly completely ionized barium plasma 1.0 m long and 5 cm in diameter. The confining magnetic field was 4 kG. Plasma density was inferred from use of a Langmuir probe in conjunction with the angle of propagation of a lower hybrid test wave with respect to $\mathbf{B}_0$ ($\theta \approx \omega/\omega_{pe}$). Electron temperature was estimated with a Langmuir probe. The ion properties were measured with the laser-induced fluorescence phase-space diagnostic.

The coordinate system used for measurements and display has $\mathbf{B} = B_0\hat{\mathbf{z}}$. The x-y plane is perpendicular to the magnetic field, with the origin at $r=0$ of the cylindrical plasma. Thus, the ion Larmor orbit is such that the ion angular momentum projection on the z axis is negative. All measurements shown in the accompanying figures were taken from scans along the x axis, holding y and z constant, collecting v_y-dependent information. This means that the displayed data are $f_i(x, v_y, t)$.

For circumstances of cylindrical symmetry, such as the application measured here, these data may yield the f_i at other x,y positions through rotation about the symmetry axis. Also, for periodic phenomena involving ion Larmor motion, $f_i(x, v_x, t)$ are obtained by examination of $f_i(x, v_y, t+3\pi/2\omega_{ci})$. Some carefully resolved periodic phenomena involving ion Larmor motion then can yield $f_i(x,y,v_x,v_y,t)$. The assistance of symmetry is lost in the x-z plane and a more complete set of measurements can be made and then unfolded to yield $f_i(x,y,z,v_x,v_y,v_z,t)$.[12]

An electrically conducting, variably biased button of 6 mm diam was placed in an x-y plane and centered at $x=-0.5$ cm, $y=0$ located as shown in Fig. 1. This button may be dc biased or ac driven to produce an electrostatic ion cyclotron instability. Coherent ion response to this instability has been observed.[15] This instability creates perturbations in phase space, details of which are discussed below. Figure 2(a) shows measurements of two quadrants of the x-v_y plane at a fixed time when a small-amplitude ($e\phi/T < 1$) ion instability is generated by an electron current drawn to the button. Because of the symmetry of the driving system and the ion Larmor orbit, the remaining two quadrants may be surmised by a mapping of

$$f_i(x, v_y, t) \rightarrow f_i(-x-1, -v_y, t),$$

i.e., a flipping of each point through $x=-0.5$, $v_y=0$. Contours of equal phase-space density are drawn in Fig. 2(a) as a function of x and v_y. The peak value of the phase-space density in the plot occurs along the $v_y=0$ axis outside of the button region and has a value of 2.8×10^4 sec cm^{-4}. The contours follow fractions of this value and from large v_y to $v_y=0$ (top to bottom in the figures) occur progressively at 5%, 10%, 15%, 20%, 30%, 40%, 50%, 60%, 70%, 80%, and 90% of the peak value of 2.8×10^4 sec cm^{-4}. For a distribution function which is isotropic and homogeneous in physical space, contours parallel to the x axis would result.

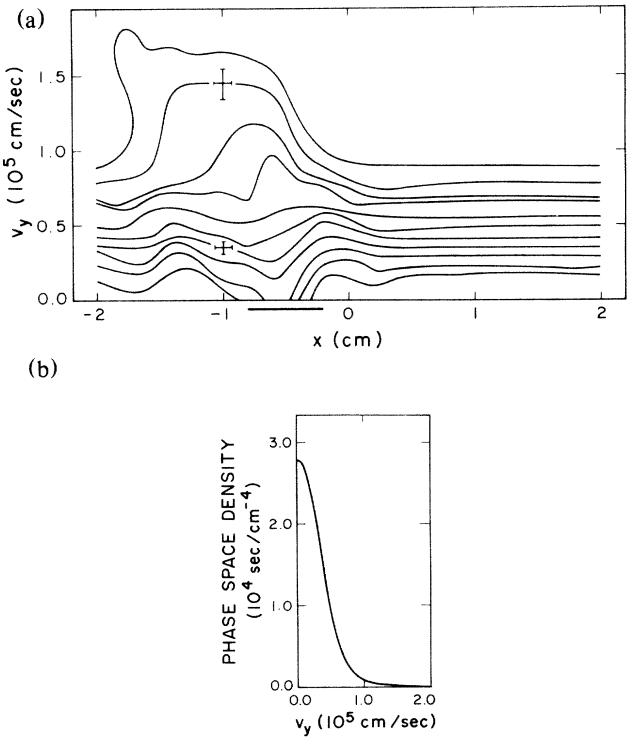

FIG. 2. (a) Phase-space density in two quadrants of the x-v_y plane showing undisturbed distribution on the right and perturbation from small-amplitude instability on the left. The bar below the horizontal axis indicates the extent of the instability source driving function (button location) in x. From top to bottom the contours represent the 5%, 10%, 15%, 20%, 30%, 40%, 50%, 60%, 70%, 80%, and 90% of the peak value of 2.8×10^4 sec cm^{-4}. (b) Phase-space density for $v_y \geq 0$, $x=$ const, obtained from a laser scan in the region of plasma $x \geq 0.5$ cm showing the Maxwellian nature of undisturbed ions.

This is seen on the right of Fig. 2(a). Figure 2(b) shows a typical data scan of f_i ($x = \text{const}, v_y$) taken at $x > 0.5$ cm which corresponds to a vertical cut through the right-hand region in Fig. 2(a) and one can see how a homogeneous, isotropic Maxwellian would give the parallel contour pattern displayed on the right-hand side of Fig. 2(a). This figure also shows that ions whose orbit passes through the button current channel are affected by the instability for this experiment. Hence, perturbations to the phase-space density are observed only to the left in the figure. Ions whose paths may have $x > x_{\text{button}}$ will display phase-space changes for $v_y < 0$ only, consistent with the mapping among quadrants in the x-v_y plane (to see this, consider the Larmor orbits of various ions which pass through the button current channel, where they cross the x axis again, and the instantaneous v_y at these points).

Time evolution of phase-space density is shown in Fig. 3. The ion wave (with $e\phi/T < 1$) frequency was about $\omega = 3.2 \times 10^5$ sec^{-1}. A sampling window in time corresponding to one-tenth of a wave period allowed measurements of phase-space density to be followed through a wave period. Displayed in Fig. 3 are four plots of phase space taken at different phases during a wave period with $\delta\theta \sim \pi/2$ between consecutive plots. As expected, the ions show a coherent response tied to the wave phase. There is a density reduction in the current channel corresponding with a density rise outside the channel which is most pronounced for $\theta = 3\pi/2$. There is a "tongue" of phase-space density oscillating at ω and reaching out in x and v_y. By calculating Larmor radii for ions passing through the button channel one may conclude that the tongue consists of particles which are near $v_x = 0$ both when in the button channel and at the observation point outside the channel. Additional observations[16] on the distribution function measured parallel to $\mathbf{B}_0$ show a phase-resolved v_z bunching of the ions in the z direction. To generalize the concept of bunching, this tongue is a measurement of phase-space bunching in four dimensions, three velocity dimensions and one spatial dimension. We note that more dimensions can be examined when tomographic techniques are applied.[12] As examples, particle bunching is thought to play a role in such wave-particle phenomena as the two-stream instability and pulsar radiation mechanisms.[17] Additionally, there is some heating within the current channel. As an aside, properties such as the energy density $u(x,t)$ and the velocity-dependent energy density $u(x, v_y, t)$, momentum density, etc., may be calculated from this type of figure.

When the wave was driven nonlinearly to large amplitudes ($e\phi/T >> 1$) the phase-space plot shown in Fig. 4 was obtained. This phase-space density was

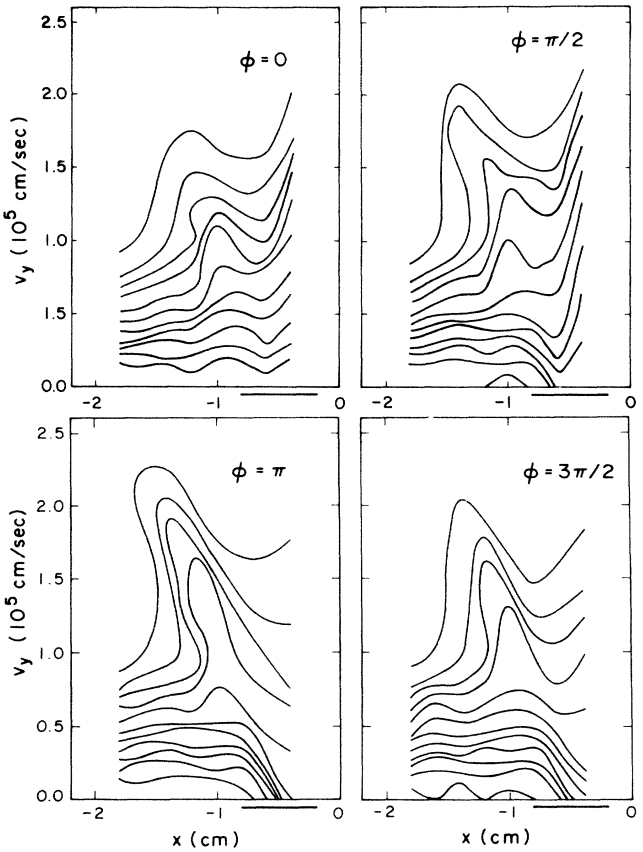

FIG. 3. Phase-space density at increasing phases during one period of a small-amplitude instability. The bar below the horizontal axis indicates the extent of the instability source driving function (button location) in x. The contours have the same definition as in Fig. 2(a).

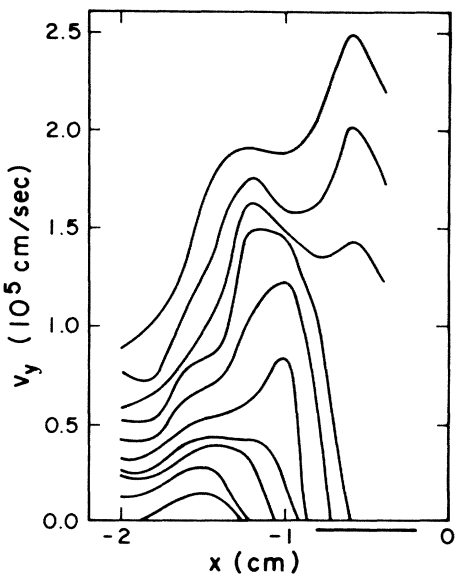

FIG. 4. Nonlinearly driven phase-space response, essentially independent of wave phase, i.e., time independent. The bar below the horizontal axis indicates the extent of the instability source driving function (button location) in x. The contours have the same definition as in Fig. 2(a).

found essentially to be independent of wave phase (in contrast to the case $e\phi/T < 1$). The ion response in Fig. 3 was coherent and could be time resolved, whereas for the conditions of Fig. 4 no coherent ion response could be found within the diagnostic time resolution. Hence, at some intermediate wave amplitude not studied in this experiment the ion response changed from coherent to turbulent. For this large-amplitude case, the waves in the plasma were comprised of electrostatic ion cyclotron waves above many of the ion cyclotron harmonics, but the role of the amplitude and spectral widths of these waves has not been determined yet. The button bias does have a strong effect on the parallel drift of the ions. The average parallel drift speed of the ions is reduced in the button channel[16] by the wave. The density reduction in the channel is due to a raising of plasma potential in the channel and to radial outflow of ions from the channel, as evidenced in the figure. Some particles are accelerated to large $|\mathbf{v}|$ by the potential oscillations in the channel. Figure 4 shows measurements of v_y acceleration creating a tail in $f(v_y)$ in the channel. These particles have a Larmor diameter of greater than 1.5 cm (bringing them near the plasma edge) and also would be found in the phase-space quadrant of positive x and negative v_y. An enhanced density of fast particles is seen for $-1.9 \lesssim x \lesssim -1.0$ cm which corresponds to particles with negative v_y in the channel orbiting to x values where they have a positive v_y on the x axis. For similar tail particles to those shown in the channel, but with negative v_y in the channel, a change in phase-space density would be expected near $x = -2.4$ cm. Port restrictions on the vacuum vessel restrict the laser diagnostic to $|x| \lesssim 2.0$ cm, and so optical information near the edge of the plasma is unavailable for this experiment.

In summary, direct, nonperturbing measurements of phase-space density integrated over two velocity components have been made in an experiment. Time, space, and speed resolution of 2×10^{-6} sec, 10^{-3} cm^3, and 3×10^3 cm/sec, respectively, have been obtained. Measurements were made of unperturbed phase space, along with linear and nonlinear wave effects. Density reductions and enhancements were observed as well as particle acceleration. Coherent and incoherent responses showed linear particle responses and that a transition to turbulence occurred. Phase-space particle bunching was seen.

The authors thank Dr. Nathan Rynn for discussions and Mr. Stacy Roe for technical assistance. This work was supported by National Science Foundation Grant No. PHY-8306108.

[1]S. J. Zweben, Phys. Fluids **28**, 974 (1985).

[2]R. L. Stenzel, W. Gekelman, and N. Wild, Phys. Fluids **26**, 1949 (1983).

[3]P. F. Mizera *et al.*, J. Geophys. Res. **86**, 2329 (1981).

[4]R. C. Davidson, *Methods in Nonlinear Plasma Theory* (Academic, New York, 1972).

[5]S. P. Gary, M. F. Thomsen, and S. A. Fuselier, Phys. Fluids **29**, 531 (1986).

[6]M. J. Feigenbaum, J. Stat. Phys. **19**, 25 (1978).

[7]S. Newhouse, D. Ruelle, and F. Takens, Commun. Math. Phys. **64**, 35 (1978).

[8]M. Kono, Phys. Fluids **28**, 1494 (1985).

[9]T. H. Dupree, Phys. Fluids **15**, 334 (1972).

[10]T. H. Dupree, Phys. Fluids **25**, 277 (1972).

[11]F. Doveil, Phys. Rev. Lett. **46**, 532 (1981).

[12]R. Koslover and R. McWilliams, University of California, Irvine, Technical Report No. 86-18, 1986 (to be published).

[13]D. N. Hill, S. Fornaca, and M. G. Wickham, Rev. Sci. Instrum. **54**, 309 (1983).

[14]N. Rynn, Rev. Sci. Instrum. **35**, 40 (1964).

[15]R. A. Stern, D. N. Hill, and N. Rynn, Phys. Rev. Lett. **47**, 792 (1981).

[16]A. Lang, Ph.D. thesis, University of California, Irvine, 1984 (unpublished).

[17]F. C. Michel, Rev. Mod. Phys. **54**, 1 (1982).